Preferred citation: T.C. Maloney and H. Paulapuro. Thermoporosimetry of Pulp Fibers. In **The science of papermaking**, *Trans. of the XIIth Fund. Res. Symp. Oxford, 2001*, (C.F. Baker, ed.), pp 897–926, FRC, Manchester, 2018. DOI: 10.15376/frc.2001.2.897.

THERMOPOROSIMETRY OF PULP FIBERS

Thad C. Maloney[1] *and Hannu Paulapuro*[2]

[1]JM Huber Finland Oy, Hamina, Finland
[2]Helsinki University of Technology, Espoo, Finland

ABSTRACT

This paper covers the use of thermoporosimetry to measure the pore size distribution (PSD) of pulp fibers. Thermoporosimetry is based on the melting temperature depression of an absorbate in a porous structure. A discreet or "step" melting procedure, rather than the usual continuous method, is used to melt the absorbate. This method eliminates thermal lag and gives the high temperature accuracy required for measuring large pores.

Measurement of water-saturated chemical pulp fibers using this technique, combined with solute exclusion, indicates a bimodal distribution of cell wall pores. The interpretation of data from water-saturated fibers is complicated by several factors: 1) distortion of the cell wall by ice crystal growth; 2) the depression of water's melting temperature by osmotic pressure; and 3) inadequate range to cover the larges pores. One way to correct these problems is by replacing the water with cyclohexane. The major disadvantage of this approach is that the cell wall contracts in cyclohexane and its pore structure may change in other ways which are not understood.

Like water, the cyclohexane analysis shows a bimodal distribution of pores. The smaller pores, "micropores", are less than about 5 nm in diameter, the "macropores" are about 15–700 nm. It was found that there is a quantity of cyclohexane in the cell wall which does not freeze. Analysis of nonfreezing cyclohexane indicates a surface area of about 400 m^2/g for kraft pulp. The

cyclohexane method is very suitable for studying beating, which primarily involves the opening of larger pores.

INTRODUCTION

Differential scanning calorimetry (DSC) is a popular method for the evaluation of thermal transitions in a wide variety of materials. In DSC, the temperature of a sample can be controlled according to a preset program and the power input or output from the sample is measured. Melting, freezing and other first order transitions show up as peaks on the temperature-power plot.

One common use of DSC is for the measurement of bound water in hydrated polymer systems. In this application, individual fractions of bound water can be quantified from the differences in their thermodynamic behavior. Nonfreezing water is the fraction that does not show any first order transition. This type of water has been reported for many types of materials including pulp fibers [1] and isolated wood polymers [2]. Indeed, it appears that nonfreezing water is a universal feature of hydrated systems. Other fraction(s) of bound water are detected as separate peak(s) on the DSC melting plot. In many cases, one type of this "freezing bound water" is found [3–5], but in some systems multiple peaks are detected [6].

The use of DSC in pulp fiber science has been rather limited until recent times. One of the pioneers in this area is T. Hatakeyama, who analyzed the melting and freezing transitions of water in celluloses and identified two types of bound water: nonfreezing water and freezing bound water [3,7]. Berthold and Salmen used DSC to measure the bound water in hemicelluloses [2]. They concluded that the swelling of hemicelluloses is largely determined by the type and amount of bound water adsorbed on different hydration sites. There have been somewhat fewer DSC studies of pulp fibers [1,8,9]. Although these have certainly been of interest, they have not come close to realizing the full potential of this technique.

These earlier studies encouraged the authors to undertake a systematic DSC study of pulp fibers. This undertaking was originally an attempt to quantify bound water for dewatering studies, but has more recently focused on analysis of the fiber pore structure.

MEASUREMENT PRINCIPLE

The purpose of this paper is to show how DSC can be used to measure fiber pore size distribution (PSD). The measurement technique, called thermoporosimetry, is based on the fact that the melting point of an absorbate varies inversely with the size of the pore which contains the absorbate. Thermoporosimetry has been used to evaluate many types of materials including: polymer composites [10], glass [11], porous carbons [12] and synthetic fibers [13]. Despite the continued interest in this field, thermoporosimetry has not gained the popularity of the classic pore measurement techniques: mercury intrusion and nitrogen sorption.

One of the main problems with thermoporosimetry is thermal lag. This means the temperature difference between the sample and the measurement sensor, which is located just below the sample. This problem can be seen in Figure 1, which shows the DSC melting curves for some water-saturated porous materials at a constant 5°C/min heating rate. For the samples with bigger pores, including pulp fibers, the thermal lag causes the peaks to overlap, making direct evaluation impossible. For the porous glass with relatively small pores (12 nm), the melting depression is large enough that the peaks are completely separated. The amount of pore and bulk water in the sample can be calculated by integrating each peak. Although thermal lag can be minimized by using small samples and low heating rates, it can not be eliminated in a constant rate heating program. Clearly, this limits the use of this approach to measure larger pores.

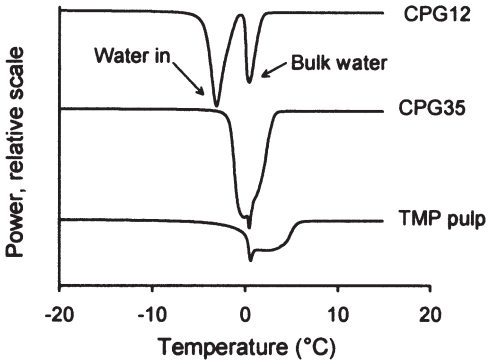

Figure 1 DSC endothermic curves for some water-saturated porous materials. CPG = controlled porous glass, followed by the nominal pore diameter in nanometers. 5°C/min heating rate.

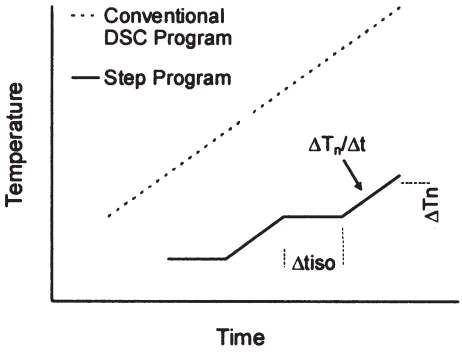

Figure 2 Schematic of step melting method and a conventional DSC measurement. The measurement parameters are: Δt_{iso} = length of isothermal segment, ΔT_n = size of step, $\Delta T_n/\Delta t$ = heating rate.

A good way to eliminate the thermal lag is to replace the conventional constant heating rate program with a "step" program in which the sample is heated in discreet increments [14]. At each step, the temperature is held constant until thermal equilibrium is reached. The step program, illustrated in Figure 2, can be adjusted according to the specific sample requirements. The size of the step is set to give suitable resolution. The length of the constant temperature period ("isothermal segment") should be sufficient for melting to reach equilibrium. The heating rate between steps is normally 1°C/min. This gives a reasonably fast measurement and large signal, but is not large enough to cause major disturbances in the signal as the mode of operation switches from isothermal to dynamic heating and back.

The melting temperature depression (ΔT) can be converted to pore diameter (D) through application of the well-known Gibbs-Thomson equation, which for fully wetted cylindrical pores is:

$$D = \frac{4VT_0\sigma_{ls}}{H_m\Delta T} = \frac{k}{\Delta T} \tag{1}$$

where V is the molar volume, σ_{ls} is the interfacial tension between solid and liquid, T_0 is the normal melting point and H_m is the latent heat of melting. In the working form of the Gibbs-Thomson equation, k = 43 nm.°C for water [4]. As Figure 3 shows, the step thermoporosimetry method is in good agreement with mercury porosimetry. Because the step method gives excellent temperature accuracy (±0.02°C) it is also suitable for the evaluation of

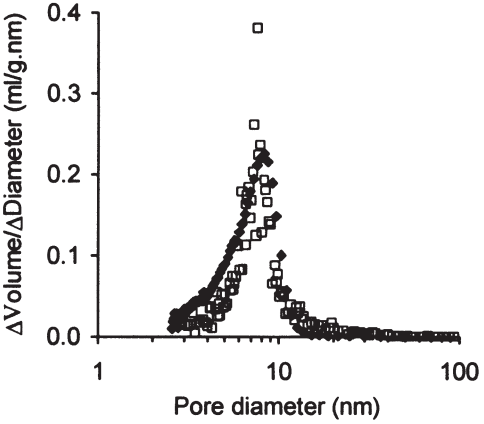

Figure 3 Comparison of Hg porosimetry (open symbols) with thermoporosimetry for porous silica. Derivative function.

relatively large pores. The upper limit of the measurement depends on the type of material being evaluated and the amount of error which is acceptable. For water-saturated materials, in the best cases, pores as large as 400 nm can be measured. For pulp fibers, 200 nm is a more realistic estimate.

Pulp fibers are very challenging to measure with thermoporosimetry. One problem is that they require both a large measurement range, to cover the broad PSD, and high resolution, to measure large pores. This can be achieved by using a program in which the step size decreases as temperature increases. An example of the melting curve for water-saturated pulp using this type of program is shown in Figure 4.

The area under the step melting plot includes a contribution from both sensible and latent heats. Only the latent heat is needed to calculate the amount of melted water. The area under the first step is used to measure the sample's sensible heat gain, so it should be at a low enough temperature that no melting occurs. In Figure 4, the first step begins at –25°C and ends at –23°C. The heat of the first step, H_{T1} is subtracted from the total heat of each other step, H_{Tn} after accounting for the size of the step, in order to calculate the latent heat, H_{Ln} according to

$$H_{Ln} = H_{Tn} - H_{T_1} \frac{\Delta T_n}{\Delta T_1} \tag{2}$$

where ΔT_1 is size of step 1 and ΔT_n is the size of step n. Equation 2 applies

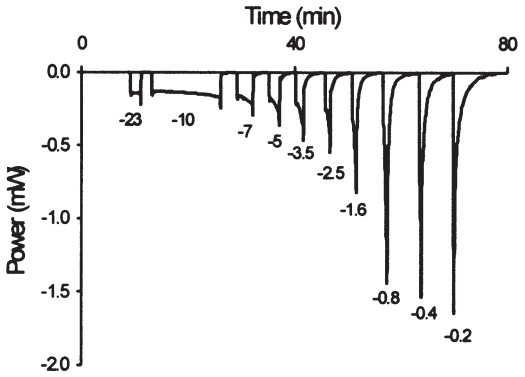

Figure 4 Example of step melting curve used to calculate pore size distribution of water-saturated pulp. The temperature at the end of each step, in °C, is marked.

only when the heating rate between each step is the same. H_L can be converted to pore volume by Equation 3. Measurements of porous silica with known pore volumes [14] indicate that the temperature dependence of H_L is small and can be neglected. Therefore, the volume of pores in each temperature interval (V_n) can be calculated by

$$V_n = \frac{H_{Ln}}{H_m W} \tag{3}$$

where W is the dry mass of the sample.

Accurate calibration is essential in thermoporosimetry. Fresh, twice distilled water and 99.9999% pure mercury were used as calibration standards. The temperature calibration was done using a step program with 0.02°C steps and 10 min isothermal segments. The program was run over the range of the melting transition. The temperature at which all the material melts was taken as the calibration temperature: 0.00°C for water and –38.80°C for mercury. The melting of water and mercury at a constant 5°C/min heating rate was used for heat calibration. H_m for water is 334 J/g and for mercury 11.4 J/g. The sample size was 2 mg for water and 20–30 mg for mercury. The sample pan holding mercury was autoclaved to form an oxide-hydroxide layer which prevents reactions between the mercury and aluminum. A Mettler 821^e DSC equipped with an intracooler was used. Its temperature accuracy in step melting is about ±0.02°C and the heat accuracy 1–2%. N_2 carrier gas set at 100 ml/min was used.

PULPS AND SAMPLE PREPARATION

Most of the following experiments were made with the fiber fraction (R50) of 4 commercial pulps: unbleached thermomechanical spruce pulp (TMP), never-dried bleached softwood kraft pulp (BSW), BSW pulp dried at room temperature and rewetted (BSW-dried) and never-dried BSW pulp beaten 10,000 revolutions in a PFI mill (BSW-beaten). For this pulp the fibers were separated after refining. The pulps were thoroughly washed in deionized water, followed by washing in 0.001M HCl. The pulps were washed finally in twice-distilled water.

Pulps for DSC measurements with a cyclohexane (chex) absorbate were prepared by a solvent exchange procedure. The solvent exchange was done in the following sequence: water-methanol-acetone-chex. The exchange was done by washing the pulp thoroughly in fresh, dry solvent then sealing the pulp in a jar with added zeolite to adsorb water. The same procedure was repeated the next day, or the following Monday. Each exchange was done 7 times for a total of 21 exchanges.

The water-saturated DSC samples were prepared by forming a 50 g/m^2 filter cake which was adjusted to 2.5 g/g moisture content. The pulp sheet was stored in an air-tight plastic bag. Round samples 5.5 mm across were cut from the sample and sealed in a DSC aluminum pan. The chex DSC samples were made by adjusting the cyclohexane content of the pulp to 4 g chex/g solids. A small clump, 2–5 mg, of the chex-saturated fibers was quickly taken with tweezers and sealed in the DSC pan. The cyclohexane content of the pulp was kept relatively high to prevent the fibers from drying out in the few seconds it took to seal these in the pan. After measurement, a small hole was punched in the pan and the sample was dried at 105°C for four hours before cooling in a dessicator and weighing to an accuracy of ±0.001 mg.

PSD OF FIBERS MEASURED IN WATER

While the focus of this paper is on measurement with a chex absorbate, a short review of the earlier reported [15] water-based results is included here. The PSD of kraft fibers in water is shown in Figure 5. The amount of non-freezing water is included. This is shown by a dotted line in the left side of the distribution. The total amount of water in the cell wall, the fiber saturation point (FSP), is marked in the figure by a straight line on the right side of the distribution. The FSP in this figure was measured by solute exclusion [16]. The effect of bulk water melting was accounted for by separately measuring a sample of bulk water and subtracting its melting from the pulp's PSD [17].

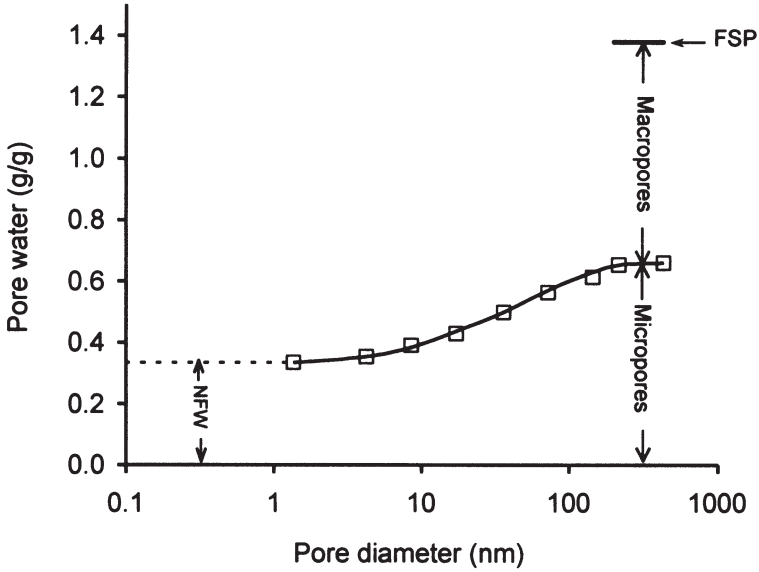

Figure 5 The pore size distribution of bleached softwood kraft fibers (Na^+ form) from thermoporosimetry. The figure shows the method for classifying fiber pores into micropores and macropores. The position of the bar used to indicate FSP is arbitrary and does not relate to the size of the probe dextran molecule [15].

Figure 5 shows that about half the water in the cell wall is not included in the thermoporosimetric measurement. We have proposed that this water is held in large pores outside the measurement range. These pores are called "macropores". This term was coined many years ago by Stone and Scallan to describe a family of large cell wall pores which do not collapse on solvent exchange drying [18]. The relatively smaller pores, which are detected with DSC, are called "micropores".

The micropores hold two fractions of water: nonfreezing water (NFW) and freezing bound water (FBW). The macropores contain bulk water (BW). The water in micropores is sometimes called the total bound water (TBW). The relationship between the water fractions is given in eq. 4 and 5.

$$\text{FSP} = \text{NFW} + \text{FBW BW} \tag{4}$$

$$\text{TBW} = \text{NFW} + \text{FBW} \tag{5}$$

There are several possibilities for measuring freezing bound water. One way

is to read it directly from the PSD diagram. However, if the entire PSD is not needed, a simpler method is to freeze, melt and then refreeze the pulp sample at a temperature just below the bulk melting. In this study, the following 5 step program was used: a) +3°C to −30°C, b) −30°C to −0.2°C, c) hold at −0.2°C for 10 minutes d) −0.2 °C to −30°C e) −30°C to +25°C. Heating and cooling rate was 5°C/min. Integration of the freezing peak in step "d" is used to calculate freezing bound water. It is important to integrate the freezing peak in such a way that it only includes the latent heat. Nonfreezing water was calculated by subtracting the freezing water (peak "e") from the total water content of the sample.

The Freezing bound water is determined at −0.2°C because this is the highest temperature where bulk water displays negligible melting and where the accuracy remains acceptable. In earlier work, this temperature was reported to be −0.3°C [19]. However, measurements on a more accurate DSC allow us the revise this estimate to 0.2°C.

PROBLEMS OF PULP FIBER MEASUREMENT

In general, the findings in our water-based thermoporosimetry study [15] were self-consistent and in agreement with earlier work on fiber pore structure [18]. Despite this encouraging result, it is apparent that pulp fibers present special problems for thermoporosimetry. The most important of these, as we see them, are summarized in the following list.

1 The freezing of pulp fibers has an unknown and potentially destructive effect on the cell wall.
2 The Gibbs-Thomson equation assumes that the melting temperature depression is caused by the pressure difference across a curved interface. It does not account for other factors which reduce the melting temperature of the absorbate. In pulp fibers, water's melting point is also reduced by the partial dissolution of cell wall polymers and by the presence of ions.
3 The macropores are not explicitly detected with DSC. Their existence is inferred from comparison of the thermoporosimetry data with the FSP. It would be desirable to extent the range of the measurement to cover the macropores.
4 The size of the cell wall pores which is measured with thermoporosimetry is larger than from other techniques.

In this paper, the possibility to eliminate or minimize these problems is

examined. As a first step in this direction the effect of freezing on pulp fibers is considered.

FREEZING PULP FIBERS

It is well known that the properties of chemical pulps change upon freezing [20]. In fact, freeze damage to biological tissues is a central problem in food storage and in cryogenic preparation of samples for microscopic study. An excellent review of the latter subject is given by Robards [21].

Freeze damage to biological materials is the result of either internal or external ice crystal growth. If crystals form within a cell, the growing crystals can rupture and distort internal structures. Ice crystals on the outer surface dehydrate the cell as water diffuses to the growing crystals. The type and extent of cell damage depends on the cooling rate. This is mainly because the size of crystals varies inversely with the cooling rate. If the cooling rate is extremely high then water does not freeze at all, rather it solidifies in a glassy state (vitrifies). In another study [21], it has been shown for yeast cells that slow freezing (1 K/sec) resulted in external crystal growth and cell dehydration. At a higher cooling rate, (10 K/sec) internal crystal growth and corresponding damage was evident. In very fast freezing, (1000 K/sec) both types of damage were avoided.

In the present study, an attempt is made determine the mechanism of freeze damage in pulp, and to see if this damage can be avoided. In this experiment, freeze damage is measured by the loss in fiber swelling (FSP). The loss in FSP is often used to measure the extent of hornification when a pulp is dried. Likewise, freezing is a dehydration process and can "hornify" a low-yield pulp. Certainly, this is the case when crystal growth on the outer fiber surfaces robs the fiber wall of water. It also seems possible that internal ice crystal growth could dehydrate neighboring regions of the cell wall and cause a loss of fiber swelling.

In Figure 6, the FSP for hardwood kraft pulp is shown as function of time frozen. There is a substantial loss in FSP compared to the never-frozen sample, and this increases with time. The ice crystals continue to grow even when the sample is frozen. One reason for this is that the nonfreezing water is fairly mobile even at low temperatures. A well-known consequence of this phenomenon in nature are the undulations, commonly called "frost heave", which develop in frozen soil [22]. There is a greater loss in FSP at higher temperatures. This is probably caused by faster water diffusion and crystal growth.

An experiment was performed to find out if the loss of FSP is due to internal or external crystal growth. This was done by freezing some kraft

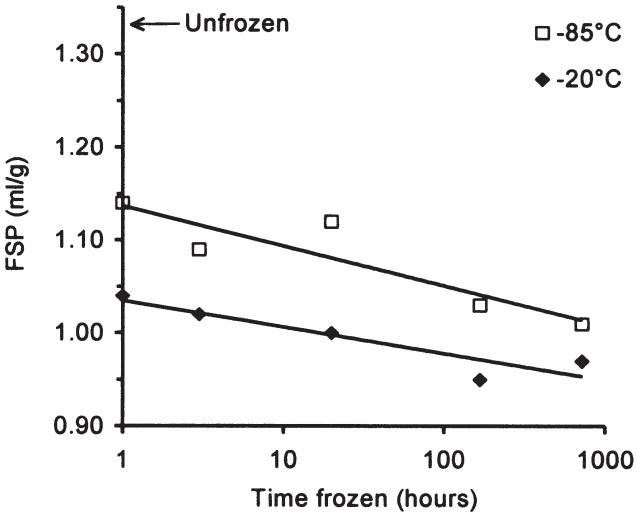

Figure 6 The loss of FSP over time for never-dried bleached kraft hardwood pulp (H^+ form) frozen at moisture content = 2.5 ml/g.

fibers in a solution of 70,000 Dalton dextran. The dextran molecules are too large to penetrate into the cell wall. The depression of the external solution's freezing point is expected to force crystallization to begin inside the cell wall and thus prevent dehydration. As Table 1 shows, the dextran completely prevented the loss in FSP. This confirms our belief that the hornification in freezing is caused by the movement of water from the inside to the outside of the fiber wall.

Table 1 Effect of freezing conditions on FSP (ml/g) of pulp fiber fractions.

Freezing conditions	TMP	Lightly beaten BSW[2]
Never frozen or dried	0.58	1.28
Quick liquid N_2 freeze		1.19
–20°C, 38 days in water	0.61	0.86
–20°C, 38 days in 10 % T70 dextran[1]		1.28
Air dried, never frozen	0.56	0.64

[1]70,000 Dalton dextran. [2]Bleached softwood kraft.

Table 1 shows that freezing has no impact on the FSP of mechanical pulp. This is probably because the presence of lignin and hemicelluloses between microfibrils prevents hornification. The fact that the pore volume from thermoporosimetry equals the FSP, as found previously [15], shows that mechanical pulps do not dehydrate in freezing.

In addition to external crystal growth, it seems likely that the growth of crystals inside the cell wall can bias the thermoporosimetry measurement. While it is not an easy task to prove this, some light can be shed on this issue with the following experiment. Pulp fibers were frozen, then heated to –0.2°C below the bulk melting temperature and held at constant temperature for 10 minutes. This allows at least some of the water in the cell wall to melt, while the water outside the fibers remains frozen. This cycle was repeated 10 times and the amount of freezing bound water measured from the freezing curves. If there is damage to the pore network from crystallization this should be reflected by a change in the amount of freezing bound water as the freezing/melting cycle is repeated. The experiment was also done with cyclohexane

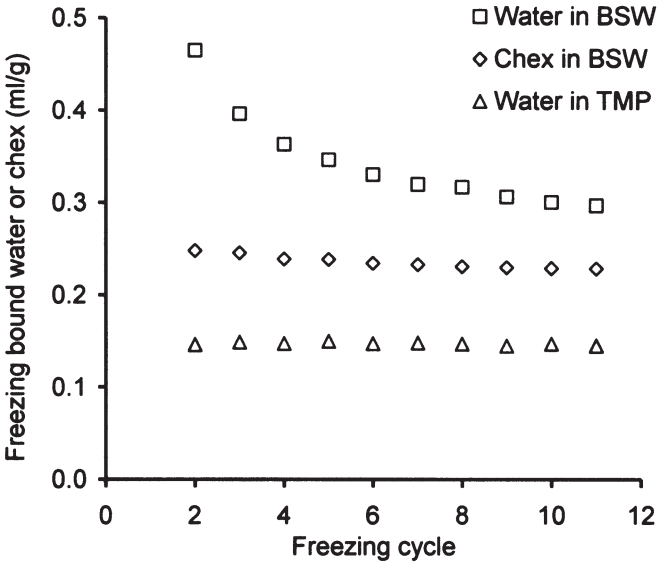

Figure 7 The amount of the freezing bound fraction, for either water or chex, after repeated freezing cycles. The sample was completely frozen, then melted at –0.2°C below the bulk melting temperature in repeated cycles. Note that super-cooling prevents the measurement of the freezing bound fraction in cycle 1.

(chex) as an absorbate. The use of chex in thermoporosimetry will be discussed later.

The results from this experiment are shown in Figure 7. The amount of freezing bound water in the BSW fibers decreases in repeated freezing, for TMP it does not. It appears that the rigid mechanical pulp fiber can withstand crystal growth, while the softer chemical pulp fiber can not. When the BSW fiber in chex is subjected to freezing cycles, there is no evidence of pore damage; the amount of freezing bound chex remains nearly constant. If there are distortions to the fiber pores when chex crystallizes then these are reversible; suggesting any such distortions are small.

In Table 1, the results from quench freezing the fibers in liquid N_2 are shown. Freezing in this way causes a fairly small loss in FSP compared to relatively slow freezing at –20°C. This shows that fast freezing can reduce the pore damage of chemical pulps. This result encouraged us to pursue quench cooling in DSC measurements. In these experiments the sample, sealed in an aluminum pan, was plunged into N_2 at its boiling point or into different organic solvents at –80°C. After quench cooling the sample was inserted into the DSC measurement chamber. Unfortunately, the quench cooling did not result in a significant change in the PSD. This is probably because the cooling rate was insufficient to affect the crystal growth and dehydration processes.

CYCLOHEXANE AS A THERMOPOROSIMETRY ABSORBATE

One way to improve the thermoporosimetric measurement is to use a solvent that has more favorable properties than water. A suitable solvent should have at least the following characteristics:

1 Not swell pulp or otherwise interact strongly with the fiber components.
2 Not display complex melting behavior e.g. polymorphism.
3 Have a melting point preferably between –20°C and + 20°C. The lower temperature limit is because the minimum operating temperature of the DSC was –70°C. The upper limit is so the solvent will be liquid at room temperature to facilitate solvent exchange.
4 Have a high melting point depression (large k in Eq. 1).
5 Display minimum premelting.
6 Available in high purity.

A number of organic compounds were screened as potential absorbates. These included: benzyl alcohol, 1-octanol, n-decane, hexadecane, camphor and cyclohexane. Besides chex, all the other molecules displayed some sort of

Table 2 Comparison of cyclohexane and water as thermoporosimetry absorbates.

Property	Water	Cyclohexane
Polarity	Polar	Nonpolar
H-bonding	Yes	No
M_w (Daltons)	18	84
Specific gravity of liquid	1.0	0.78
Swells fibers?	Yes	No
Melting temperature (°C)	0	6.5
ΔT_m^5 (°C)[1]	0.1	0.1
k (nm.°C)[2]	44	117
Max pore diameter (nm)	430	1200
H_m (J/g)[3]	334	32
Min. pore diameter (nm)	1.3–3.0	3.6–7.5

[1]The temperature deviation from bulk melting where 5% of the material melts. A measure of premelting. [2]The melting temperature depression Equation 1. [3]Latent heat of melting.

complex melting behavior. This severely complicates their use as absorbates. The tendency to exhibit complex melting increases with the complexity of the molecular structure. Future studies of potential absorbates should probably focus on the simpler molecules.

Chex has many very attractive properties as an absorbate. These are summarized in Table 2. Chex is cheap and available in high purity (99.9%). It can easily be introduced into the cell wall through a solvent exchange procedure. Chex is a relatively large non-polar molecule that does not swell pulp fibers. It is expected that chex interacts weakly with cell wall components. It has been found in another study [23] that chex has behavior consistent with the Gibbs-Thomson equation.

Chex displays very little premelting. Premelting is the partial melting of a substance prior to the bulk transition. It is also called surface melting, usually with reference to the solid-vapor interface, or more generally, interfacial melting. Premelting is caused by the anomalous behavior of molecules at an interface. The surface molecules gradually loose their coherence as the temperature increases. The liquid-like layer grows in thickness until at the bulk melting temperature it encompasses the entire sample. This is obviously an energetic process and is therefore detected with DSC. The extent of premelting depends on the specific surface interactions and is greatly influenced by impurities [24]. Surface melting has been most widely studied for water [22,25,26]. In fact, the first description of the phenomenon was given by

Faraday over a hundred years ago [27]. Today, surface melting is acknowledged to occur in many if not all substances [28,29].

In this study, the constant ΔT_m^5 in Table 2 is used to quantify the amount of premelting. This is the deviation from the bulk melting temperature where the 5% of the substance melts. 5% chex will melt when the temperatures is 0.1°C below the bulk melting temperature of 6.5°C. This was determined by step melting of the bulk material. Water has the same ΔT_m^5 as chex. All other substances which were examined had much higher premelting. The melting temperature depression of chex (k) is 3x that of water. This means that pores 3 times larger can be evaluated with chex as an absorbate rather than water.

One disadvantage of cyclohexane as an absorbate is that the latent heat of melting (H_m) is about a tenth of water. This reduces the sensitivity of the measurement by a factor of ten. However, a modern DSC run under suitable conditions has a very high sensitivity. So far, the authors have not found this to be a major problem.

The chex can be introduced into the cell wall with a solvent exchange procedure. In solvent exchange, water is washed from the cell wall by a solvent miscible in both water and chex. The intermediate solvent is then removed by washing in chex. In this work two intermediate solvents were used. The washing must be adequate to completely desorb each preceding solvent. In this way, the pores in the cell wall can be filled with a solvent that does not spontaneously swell the fiber.

It is obvious that the pore structure of the cell wall in chex can not be the same as in water. The very smallest pores are accessible to water but not to chex. It is unclear how the hemicelluloses behave in the exchange. However, it seems possible that because they do not swell in a nonpolar solvent, they collapse onto the microfibril surface. Certainly, the elimination of osmotic pressure will cause a contraction in the cell wall. Despite these problems, it is our belief that, at least for some kinds of pulp, the fiber pore structure in chex in many way resembles the pore structure in water, and much is to be gained by measuring in chex.

The best application of chex-based thermoporosimetry measurements seems to be for chemical pulps and this is the emphasis of the present study. Mechanical pulps resist freeze damage and have a relatively compact pore structure which can be measured easily in water. However, for the sake of comparison a mechanical pulp is included in the present study.

CHEX AND WATER FRACTIONS IN PULP FIBERS

In this section, thermoporosimetric measurements are compared for pulps in water and chex. The exchanged pulps have fractions of chex in the cell wall analogous to the water fractions. "Nonfreezing chex" does not show any first order transition. "Freezing bound chex" is the fraction melting –0.2°C below bulk melting. "Total bound chex" is to the sum of these fractions. The word "bound" follows from the water fraction terminology. It is not meant to imply a specific chex-cellulose binding interaction.

Table 3 Water fractions in pulp fibers. The 95% confidence interval is shown where 5 measurements were done, otherwise the average from 2 measurements is reported.

Pulp	Moisture content[1] (ml/g)	Nonfreezing water (ml/g)	Freezing bound water[2] (ml/g)	Total bound water[3] (ml/g)	Bulk water in cell wall (ml/g)	Porosity (FSP) (ml/g)
TMP	2.42 ± 0.11	0.37 ± 0.03	0.19 ± 0.01	0.56 ± 0.03	0.02	0.58
BSW	2.70 ± 0.15	0.30 ± 0.02	0.41 ± 0.01	0.71 ± 0.01	0.38	1.09
BSW-beaten	2.25 ± 0.06	0.29 ± 0.03	0.46 ± 0.02	0.74 ± 0.05	0.73	1.47
BSW-air-dried	2.35 ± 0.15	0.29 ± 0.01	0.28 ± 0.01	0.57 ± 0.01	0.23	0.80

[1]Moisture content at which DSC measurement was done. [2]The water in pulp fibers melting at –0.2°C below the bulk melting transition. [3]Sum of nonfreezing and freezing bound water fractions.

Table 4 Cyclohexane fractions in pulp fibers. The 95% confidence interval is shown where 5 measurements were done, otherwise the average from 2 measurements is reported. See Table 3 for definition of terms.

Pulp	Chex content[1] (ml/g)	Non-freezing chex (ml/g)	Freezing bound chex (ml/g)	Total bound chex (ml/g)	Bulk chex in cell wall (ml/g)	Porosity (centrifuge) (ml/g)
TMP	2.67 ± 1.78	0.20 ± 0.04	0.32	0.52	~0	0.52
BSW	3.89 ± 1.20	0.52 ± 0.09	0.26	0.78	~0	0.80
BSW beaten	2.56 ± 0.84	0.47 ± 0.07	0.64	1.11	~0	1.10
BSW-air-dried	2.99 ± 0.38	0.26 ± 0.03	0.27	0.49	~0	0.46

[1]Refers to samples for the nonfreezing chex measurement. Freezing bound chex was measured from separate samples whose chex content was in the same range.

The water fractions were measured from the temperature program described in the earlier part of this paper. The FSP measured according to a modified solute exclusion method was used as the measure of porosity [30]. 5 DSC measurements and 2 FSP measurements were done per sample. The water-based measurements are summarized in Table 3. The chex fractions for the pulps are summarized in Table 4. The nonfreezing chex was measured in a similar fashion as nonfreezing water. The amount of freezing bound chex was read from the pore size distribution.

The porosity of the chex-saturated fibers was determined by centrifuging a 1700 g/m^2 pad of the pulp at 3000 g for 15 minutes. The pad was hermetically sealed in the centrifuge sample holder. Centrifuging, for example in the water retention test, can sometimes give wrong pore volumes because water is not completely removed from between the fibers or is pressed from the cell wall [31]. In this case, centrifuging probably gives a reasonable measure of porosity. The centrifugal force is sufficiently high and the pulps are fines-free, so the chex should be completely removed from between the fibers. Chex pulp pads are lighter than in water and the fibers are less swollen, so it is not expected that chex is pressed from the cell wall in centrifuging.

The water and chex fractions for the different pulps are shown graphically in Figure 8. The pore volume of each pulp in chex is substantially less than in

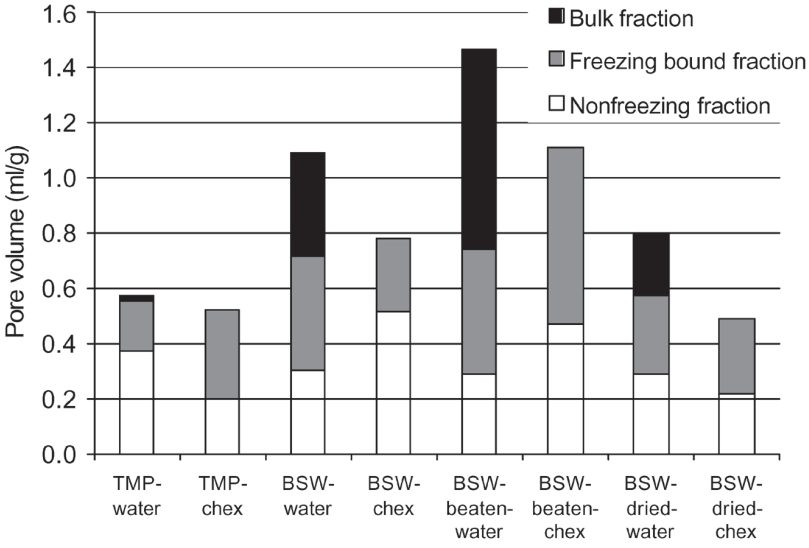

Figure 8 Comparison of water and chex fractions in pulp fibers. The height of the bar is the pore volume.

water. This is expected because the fibers are not under osmotic pressure in chex. Figure 8 shows that there is no obvious correlation between the water fraction and the chex fractions. For example, BSW has 0.30 ml/g nonfreezing water but 0.52 ml/g nonfreezing chex. On the other hand, when the water in TMP is exchanged to chex the nonfreezing fraction decreases from 0.37 to 0.20 ml/g. Table 4 shows excellent agreement between the total bound chex and the pore volume from centrifuging. This shows that there is no bulk chex inside the cell wall. This may be ascribed to three factors: 1) the fiber is less swollen in chex so the pores are smaller, 2) the measurement range is extended to 600 nm and 3) the chex does not diffuse to the outside the fiber when the sample is frozen.

PULP SURFACE AREA

It seems reasonable that the nonfreezing chex is an interfacial layer whose interactions with cellulose make freezing thermodynamically unfavorable. Data in Table 5 supports this idea by showing that the amount of nonfreezing chex increases with the accessible surface area. In this experiment, the low surface area pulp (only the outer surface accessible) was made by drying the pulp from water. The sample with high surface area was made by direct exchange to chex with no drying. The sample with an intermediate amount of accessible surface was prepared by first exchanging to pentane, evaporating the pentane and then saturating the sample with chex. Evaporation of the pentane causes partial collapse of the surface.

If the thickness of the nonfreezing layer (d) is known, it is possible to estimate the fiber surface area. d was calculated for a chex-filled porous glass

Table 5 Nonfreezing chex in unbeaten bleached birch kraft pulp with differing amounts of accessible surface area. Starting pulp was never-dried.

Sample preparation	Nonfreezing cyclohexane (ml/g)	Surface area (m^2/g)
Solvent exchanged to chex	0.60	188[1]
Solvent exchange dried, chex-saturated	0.21	56[2]
Water dried, chex-saturated	0.02	0.5–3[3]

[1]Calculated from water desorption isotherm.
[2]Measured from N_2 sorption.
[3]Estimate from literature [32,33].

Table 6 Thickness of the nonfreezing layer (d) and of monolayer (d_{mono}).

Solvent	d (nm)	d-mono (nm)	d/d_{mono} ——
water	0.43*	0.31	1.4
chex	1.3**	0.57	2.3

*Average value calculated from series of porous glass standards from D = 3–400 nm.
**Calculated from single porous glass standard with D = 7.5 nm.

standard with known surface area, assuming nonfreezing chex has the same density as liquid chex. Table 6 shows that for this system, d = 1.3 nm. It is likely that the magnitude of d depends on the specific solvent-surface interactions. Both cellulose and glass have hydroxyl-rich surfaces which interact with chex via dispersion forces. It is reasonable to assume that d for chex in glass also applies for bleached kraft fibers.

The surface area was calculated by several techniques which are compared in Table 7. Surface area was derived from the BET equation fit of the moisture desorption isotherm up to 50% RH. Surface area was also calculated from the amount of nonfreezing chex, assuming that d = 1.3 nm. Surface area was determined from the chex PSD, assuming cylindrical pores.

For BSW, surface area was calculated from the average macrofibril size, 15.3 nm, assuming square macrofibrils and neglecting bonded regions. This

Table 7 Comparison of surface area (SA) measurements.

Pulp	SA from water desorption isotherm (m^2/g)	SA from nonfreezing chex[1] (m^2/g)	SA from chex PSD[2] (m^2/g)	nonfreezing chex in PSD[2] (ml/g)	SA on outer macrofibril surface[3] (m^2/g)
TMP	220	155 ± 31	25	0.03	
BSW	183	400 ± 71	20	0.03	170
BSW-beaten	193	362 ± 54	45	0.06	
BSW-dried	173	167 ± 22	17	0.02	

[1]Calculated assuming nonfreezing chex layer 1.3 nm thick. Calculation assumes square macrofibrils.
[2]Pore size distribution of fibers in chex, assuming cylindrical pores (see Figure 11).
[3]15.3 nm average macrofibril size from atomic force microscope measurements.

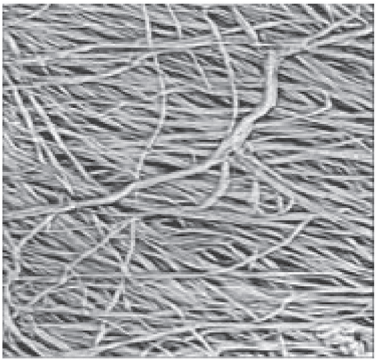

Figure 9 Phase contrast atomic force micrograph of BSW dried from chex showing macrofibrils. Image size 1 μm x 1 μm.

was determined from an atomic force microscope (AFM) tapping mode image. Figure 9 is an AFM phase contrast image from the same sample. In this paper, "macrofibril" means the aggregates of microfibrils which are commonly visible in microscopic images of pulp fibers, such as Figure 9 or [34]. "Microfibril" refers to the elementary aggregates of cellulose chains, which appear to be in the range of 1.5–6 nm [35,36].

Fiber surface area is a subject that has beguiled paper scientists for many years. There are many ways to measure surface area, and these will invariably give different results. One common method is to prepare an aerogel from the pulp, using one of several techniques, and to measure the surface area of the dry sample with N_2 sorption. The problem with the approach is that it is unlikely that the surface area is completely preserved. The surface area for chemical pulps, either solvent exchange dried or critical point dried, has been reported to be 150–200 m^2/g [33,37]. This value is very dependent on the sample preparation conditions.

Let us consider what the present measurements can add to this discussion by examining the surface area data of BSW pulp. The surface area calculated from the macrofibrils, 170 m^2/g agrees very well with the value from the moisture isotherms: 183 m^2/g. It is the authors' opinion that this agreement is fortuitous and, in fact, too low. It is very questionable if the BET equation is applicable to the water-fiber system because the surface is not already exposed, but is formed by the adsorption of water. The surface area determined from the micrograph seems likely to underestimate the total surface area because it does not include surface within the macrofibrils. The surface area calculated from the nonfreezing chex is 400 m^2/g. This is about twice the

outer macrofibril area which was calculated from the AFM micrograph. This supports the idea that a significant part of the surface is inside the macrofibrils, which agrees with the notion that these are composed of smaller fibrillar units.

MINIMUM PORE SIZE FOR FREEZING

There may be several different mechanisms that cause water or other solvents in porous materials not to freeze [8,38,39]. For example, in small pores there may simply not be enough molecules to form a crystal. As statistical mechanics has shown, crystallization requires a minimum amount of a substance. It appears that in pulp fibers a large fraction of the pores contains only nonfreezing chex. This can be shown by calculating the amount of nonfreezing chex in pores that also contain freezing chex. This is done by calculating the surface area from the PSD using the cylindrical pore model. For example, in Table 7 the surface area of pores containing freezing chex for the BSW pulp is 20 m^2/g. The nonfreezing layer for these pores is estimated to be 0.03 ml/g. Therefore the remaining nonfreezing chex, 0.49 ml/g, is in relatively small pores which contain only nonfreezing chex.

The minimum pore size for freezing was estimated by examining the DSC melting curves of water or chex imbibed in porous standards. Some examples of the melting curves are shown in Figure 10. The results summarized in Table 8 show whether or not a pore melting peak was observed. This allows one to determine the minimum pore size range required for freezing. For water this was from 1.3–3.0 nm and for chex from 3.6–7.5 nm. From knowledge of the pore volume and the amount of nonfreezing water or chex, it was determines that the pores were fully saturated in this experiment.

Table 8 Detection of pore melting peak in materials with different sized pores.

Material	Av. pore diameter (nm)	Pore peak detected? water	chex
zeolite NaY	1.3	no	no
silica	3.0	yes	no
silica	3.6	yes	no
controlled porous glass	7.5	yes	yes

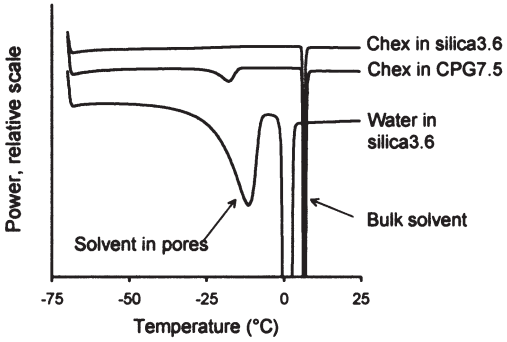

Figure 10 DSC melting curves of solvents in porous materials. CPG = controlled porous glass. The average pore diameter is indicated.

PROPOSED FIBER PSD

In this section, a hypothesis concerning the shape of the entire fiber PSD is presented. Before this, let us first consider a little more about how the fibers shrink when the water is exchanged for chex.

In Table 9, the nonfreezing chex is compared to the water in micropores for the chemical pulps. The shrinkage of the pores is corrected for by increasing the nonfreezing chex in proportion to the swelling loss after solvent exchange. After this correction, the volume of the chex-containing pores is about equal to the volume of water-filled micropores for the BSW and BSW-beaten pulps. Therefore it seems reasonable, at least for the never-dried kraft pulps, to equate the pores holding nonfreezing chex with the water filled micropores.

Table 9 Nonfreezing cyclohexane, scale up to account for reduced swelling of pulps in chex compared to water. Total bound water (volume of micropores).

Pulp	Nonfreezing cyclohexane (ml/g)	Scaled[1] nonfreezing cyclohexane (ml/g)	Total bound water (micropores) (ml/g)
BSW	0.52 ± 0.09	0.70 ± 0.12	0.71 ± 0.01
BSW-beaten	0.47 ± 0.07	0.63 ± 0.09	0.74 ± 0.05
BSW-dried	0.26 ± 0.03	0.38 ± 0.05	0.57 ± 0.01

Scaling factor = pore volume in water/pore volume in chex

For the BSW-dried pulp, the scaled amount of nonfreezing chex is lower than the micropore volume. The reason for the different behavior of this pulp is unclear. However, we will take the liberty of speculating that it has to do with the different ways that never-dried and dried pulps shrink when the water is exchanged for chex. For the BSW-dried pulp, many of the microfibrils are bonded together. This may result in more pores which are inaccessible to chex and therefore subject to collapse in the exchange.

The cumulative PSD is shown in Figure 11 for the never-dried kraft pulps in chex. This figure does not include the nonfreezing fraction. The curves do not reach a plateau because the measurement range is insufficient. However, the agreement between the thermoporosimetry pore volume, measured by the last point in the distribution, and the pore volume from centrifuging (Table 4) shows that the entire PSD has been measured. Therefore, the last point in the distribution gives a reasonable measure of the largest pores in the cell wall for the chex-saturated fibers. The slight upward curvature of the PSD is probably due to interference from premelting of bulk cyclohexane, which has not been subtracted from the PSD.

The PSD did not show any pores smaller than 16 nm for BSW pulp and about 12 nm for BSW-beaten pulp. This is significantly larger than the pores which contain only nonfreezing chex, which are less than 3.6–7.5 nm. This leads to the conclusion that the complete PSD is bimodal. This finding is in general agreement with our earlier water-based measurements. Another encouraging fact is that both water-based (Table 3) and chex-based DSC measurements (Table 4) show that beating affects mostly the volume

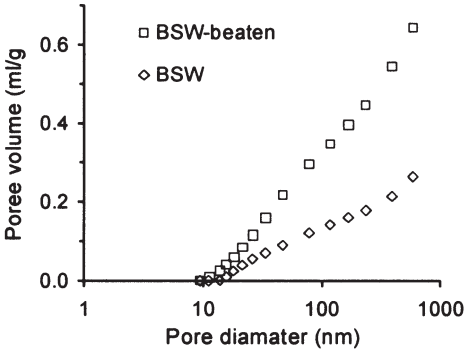

Figure 11 Measured pore size distribution of BSW and BSW-beaten pulps in chex. The volume of nonfreezing chex is not included.

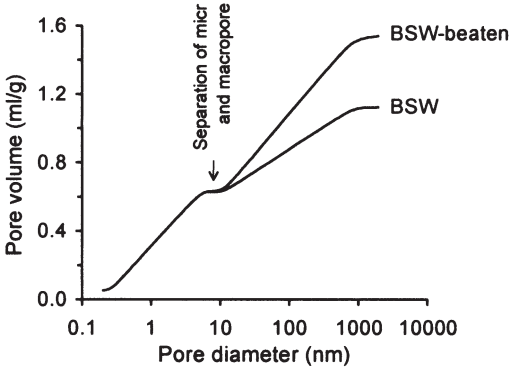

Figure 12 Hypothesized entire pore size distribution for never dried BSW fibers before and after beating.

of the larger pores; an observation supported by NMR (40) and solute exclusion measurements [16]. Figure 11 shows the great practical advantage of measuring chemical pulps in chex; macropores can now be explicitly measured.

Figure 12 shows our best estimate of the entire fiber PSD and the effect of beating on it. This estimate is based on the results in Figure 11 with the assumption that the micropores follow the same logarithmic-shaped distribution as the macropores.

It seems likely that the PSD continues down to a few nanometers and below, as found in solute exclusion [16]. In fact, it is probable that there are some pores e.g. disordered zones in the cellulose, just big enough to accommodate a water molecule, 0.3 nm. The largest pores which were found from the chex measurements were about 600 nm. If it is assumed that the pores are cylinders, which expand volumetrically in proportion to the fiber swelling, then the largest pores in water are about 700 nm.

It has sometimes been postulated [41] that there is a class of pores about 1 micrometer in diameter which are formed when the cell wall of chemical pulp delaminates in refining. In fact, the chex technique was largely motivated by our desire to in investigate this thesis. Unfortunately, the range of the measurement is not quite sufficient to measure these pores; mainly because of premelting and interference from interfiber pores. Further improvements in the method may yet allow measurement of these very large cell wall pores.

We are only beginning to understand the structural arrangement in the cell wall that leads to a bimodal PSD. Our earlier study showed that macropores

are formed in chemical pulping by the dissolution of the polymers from between the microfibrils [15]. While this description is essentially correct, it is not complete. Apparently, the process of macropore formation also involves further rearrangements of microfibrils. On one level, this probably involves the aggregation of microfibrils into macrofibrils. However, the data here suggests that there may be another level of structural hierarchy involved. This can be seen by the fact that the outer surface of the macrofibrils (170 m^2/g) is much higher than the surface area of the macropores (20 m^2/g). This implies that many of the spaces between macrofibrils are small enough to be counted as micropores. In other locations the spacing of the macrofibrils is wide enough to form macropores.

The PSD in Figure 12 is not in agreement with solute exclusion data. The thermoporosimetry measurements of BSW in chex show pores as large as 600 nm which in water might swell to about 700 nm. The largest pores found in solute exclusion are in the range of 10–30 nm [42]. We initially hypothesized that this discrepancy was caused by the presence of bottle-necks in the cell wall. Since the solute exclusion technique relies on the percolation of a probe molecule into the pores, it is sensitive to restrictions at the pore openings. In order to test this hypothesis, a thermoporosimetry hysteresis experiment was performed.

Hysteresis measurements have been done with several pore measurement techniques in an attempt to measure the shape of the pores or the interconnectivity of the network [43]. The basic principle is that the conditions for filling a pore through a bottle-neck or restriction are different than the conditions for emptying the pore. This results in a hysteresis between the filling and emptying curves which may, after appropriate mathematical analysis, be used to study the topography of the pores. Such an approach has been used in N_2 adsorption/desorption, mercury filling/emptying [43] and thermoporosimetry freezing/melting experiments [44,45].

When the absorbate in a porous sample is slowly frozen in such a manner that crystal growth starts from the outside of the sample, the solid-liquid front propagates through the pores. In the absence of restrictions, the absorbate in the pore will freeze when its temperature falls below that defined by the pore's Gibbs-Thomson radius. When the front reaches a restriction, it can not pass until the temperature drops to a low enough value. The absorbate on the other side of the restriction is thus temporarily prevented from freezing if homogeneous nucleation does not occur. In most cases super-cooling prevents this from happening. When the sample is slowly heated the process does not reverse. Melting occurs in each pore at the temperature defined by the local radius of curvature. So for a pore with a bottle-neck opening, the melting is shifted to a higher temperature than in freezing.

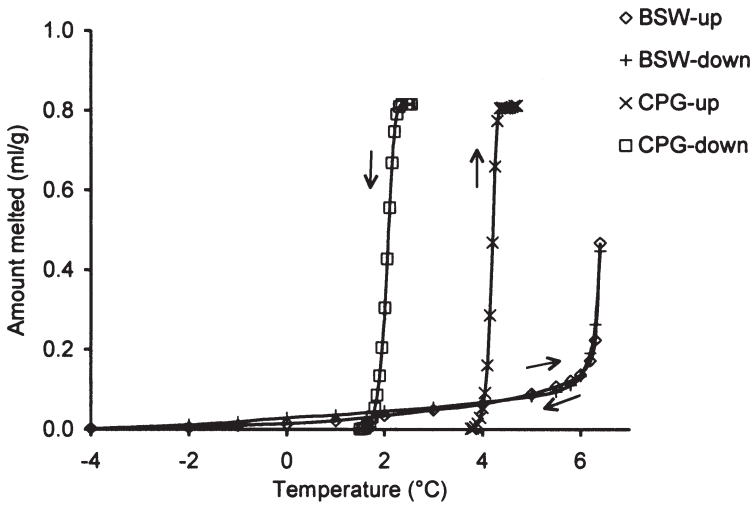

Figure 13 Hysteresis curves for BSW and controlled porous glass (D = 50 nm) in chex. The arrows indicate the direction of temperature change.

In this experiment, the hysteresis of chex-saturated BSW pulp was measured by first completely freezing the chex. The sample was then heated in steps to $\Delta T = -0.1°C$ then refrozen by "stepping down" in reverse order. This technique melts all the chex in the cell wall and avoids super-cooling during freezing because chex crystals remain outside the fibers. This same measurement was done for a sample of controlled porous glass (CPG). CPG is a type of porous silica that has a very narrow pore size distribution.

The results from this experiment in Figure 13 show no hysteresis for BSW pulp. The same result was found for BSW-beaten pulp (not shown). This indicates a well-percolated pore system free of bottle-necks. This contrasts markedly to the large hysteresis for CPG. For the CPG the entire freezing curve is shifted away from the melting curve. Hysteresis does not just occur for part of the curve. This shows that the effective bottle-necks for the CPG are on the outer surface of the porous glass particles.

Another possible explanation for the relatively large fiber pores which are found with thermoporosimetry is that this is a result of the differences in pore geometry between the calibration substance and the cell wall. In reality, the cylindrical model is a gross simplification of the pore space that does not take into account factors such as pore concavity, which is known

to influence melting behavior [46]. The development of more sophisticated pore models may help to determine if 700 nm pores really exist in the cell wall.

SUMMARY

Thermoporosimetry is an important DSC technique for the investigation of fiber pore structure. The step approach which was described in this paper is a good way to eliminate the thermal lag and to achieve the required temperature accuracy. For simple porous materials such as porous silica the application is fairly straight forward and gives good agreement with mercury porosimetry.

It is much more complicated to apply thermoporosimetry to pulp fibers. One of the major problems for chemical pulps is that freezing damages the cell wall. It was shown that this happens by transport of water to growing crystals outside the cell wall. It also seems likely that crystal growth inside the cell wall can distort the pore network. The limited range in water means that only part of the PSD can be measured. The partial solubility of cell wall components is also a problem for water-saturated fibers.

These problems can be largely solved by using a chex absorbate. Chex is non-polar and therefore does not swell the fiber, displays only a small amount of premelting and has a large melting temperature depression. The available evidence suggests that chex does not destroy the pores when it crystallizes. The range of the measurement is large enough that it covers all, or nearly all, the pores in the cell wall. When the water in the cell wall is exchanged for chex the cell wall contracts in a manner which is not easy to predict. This is a disadvantage of carrying out the measurements in chex.

In fibers, there is a large quantity of nonfreezing chex. This appears to be a layer of chex absorbed on the pore walls. In small pores, less than about 3.6–7.5 nm in diameter, the chex does not freeze at all. The smallest pores in pulp fibers containing freezing chex were found to be 12–16 nm. This implies a bimodal distribution of pores in the cell wall. This fact is in general agreement with the earlier findings from water-based measurements. For never-dried chemical pulp the nonfreezing chex, after correction for pulp shrinkage, corresponds to the volume of micropores in water. From the amount and the thickness of nonfreezing chex layer the surface area of never-dried kraft was calculated to be about 400 m^2/g. The largest pores in kraft pulp were estimated to be 700 nm.

ACKNOWLEDGEMENTS

Funding for this research was generously provided by The Finnish Academy.

REFERENCES

1. Yamauchi, T., Murkami, K., "Differential scanning calorimetry as an aid for investigating the wet state of pulp", *J. Pulp Pap. Sci*., **17**, J223–J226 (1991).
2. Berthold, J., "Water Adsorption and Uptake in the Fibre Cell Wall As Affected by Polar Groups and Structure", Doctoral Thesis, Royal Institute of Technology, Stockholm (1996).
3. Nakamura, K., Hatakeyama, T., Hatakeyama, H., "Studies on bound water of cellulose by differential scanning calorimetry", *J. Text. Inst*., **72**: 607–613 (1981).
4. Nakamura, K., Hatakeyama, T., Hatakeyama, H., "Relationship between hydrogen bonding and bound water in polyhydroxystyrene derivatives", *Polymer*, **24**: 871–876 (1983).
5. Nagura, M., Saitoh, H., Gotoh, Y., Ohkoshi, Y., "States of water in poly(vinyl alcohol)/poly(sodium L-glutamate) blend hydrogels", *Polymer*, **37**: 5649–5652 (1996).
6. Kodama, M., Nakamura, J., Miyata, T., Aoki, H., "The behaviour of water molecules associated with structural changes in negatively charged phosphatidyl-glycerol assemblies as studied with DSC", *J. Therm. Anal*., **51**: 91–104 (1998).
7. Hatakeyama, T. and Liu, Z., *Handbook of Thermal Analysis*, John Wiley & Sons: New York (1998).
8. Deodhar, S. and Luner, P., "Measurement of bound (nonfreezing) water by differential scanning calorimetry", in *Water in Polymers* (edited by: S.P. Rowland), American Chemical Society, 273–285 (1980).
9. Hatakeyama, T., Nakamura, K., Tajima, T., Hatakeyama, H., "The effect of beating on the interaction between cellulose and water", International Paper Physics Conference, Quebec, 87–91 (1987).
10. Gan, L.M., Liu, J., Chew, C.H., "Microporous polymeric composites from bicontinuous microemulsion polymerization using a polymerizable nonionic surfactant", *Polymer*, **38**: 5339–5345 (1997).
11. Ishikiriyama, K., Todoki, M., "Evaluation of water in silica pores using differential scanning calorimetry", *Thermochim. Acta*, **256**: 213–226 (1995).
12. Goworek, J., Stefaniak, W., "Study of the porosity of carbonaceous materials and organic polymers by thermal analysis", *J. Therm. Anal*., **51**: 541–551 (1998).
13. Homshaw, L.G., "Calorimetric determination of the porosity and pore size distribution PSD, effect of heat on porosity, pore form, and PSD in water-saturated polyacrylinitrile fibers", *J. Colloid Interface Sci*., **84**: 127–140 (1981).
14. Maloney, T.C., "Thermoporosimetry by isothermal step melting", ISWPC Pre-Symposium, Seoul, 245–253 (1999).

15. Maloney, T.C., Paulapuro, H., "The formation of pores in the cell wall", *J. Pulp Pap. Sci*., **2**: 430–436 (1999).
16. Stone, J.E., Scallan, A.M., Abrahamson, B., "Influence of beating on cell wall swelling and internal fibrillation", *Svensk Papperstidn*., **19**: 687–694 (1968).
17. Maloney, T.C., Paulapuro, H., Stenius, P., "Hydration and swelling of pulp fibers measured with differential scanning calorimetry", *Nord. Pulp Pap. Res. J*., **13**: 31–36 (1998).
18. Stone, J.E., Scallan, A.M., "The effect of component removal upon the porous structure of the cell wall of wood. II. Swelling in water and the fiber saturation point", *Tappi J*., **50**: 496–501 (1967).
19. Maloney, T.C., Todorovic, A., Paulapuro, H., "The effect of fiber swelling on press dewatering", *Nord. Pulp Pap. Res. J*., **13**: 285–291 (1998).
20. Kibblewhite, R.P., "Effects of pulp freezing and frozen pulp storage on fiber characteristics", *Wood Sci. Technol*., **14**: 143–158 (1980).
21. Robards, A.W., "Low Temperature Methods in Biological Electron Microscopy", Elsevier, Amsterdam et al., (1985).
22. Dash, J.G., Fu, H., Wettlaufer, J.S., "The premelting of ice and its environmental consequences", *Rep. Prog. Phys*., **58**: 115–167 (1995).
23. Jackson, C.L., McKenna, G.B., "The melting behavior of organic materials confined in porous solids", *J. Chem. Phys*., **93**: 9002–9011 (1990).
24. Beaglehole, D., "Surface melting of small particles, and the effects of surface impurities", *J. Crystal Growth*, **112**: 663–669 (1991).
25. Maruyama, M., Bienfait, M., Dash, J.G., Coddens, G., "Interfacial melting of ice in graphite and talc powders", *J. Crystal Growth*, **118**: 33–40 (1992).
26. Wettlaufer, J.S., "Crystal growth, surface phase transitions and thermomolecular pressure", in *Ice Physics and the Natural Environment* (edited by: J.S. Wettlaufer, J.G. Dash and N. Untersteiner), Springer-Verlag, 39–67 (1999).
27. Hobbs, P.V., *Ice Physics*, Clarendon Press, Oxford (1974).
28. Zhu, D-M., Dash, J.G., "Surface melting of Neon and Argon films: profile of crystal-melt interface", *Phys. Rev. Letters*, **60**: 432–435 (1988).
29. Frenken, J.W.M. and van Pinxteren, H.M., "Surface melting: an experimental overview", in *Phase Transitions and Adsorbate Restructuring at Metal Surfaces*., (edited by: D.A. King, and D.P. Woodruff.) Elsevier, 259–290, (1994).
30. Luukko, K., Maloney, T.C., "The swelling of mechanical pulp fines", *Cellulose*, **6**: 123–135 (1999).
31. Maloney, T.C., Laine, J.E., Paulapuro, H., "Comments on the measurement of cell wall water", *Tappi J*., **82**: 125–127 (1999).
32. Stone, J.E., Scallan, A.M., "A study of cell wall structure by nitrogen adsorption", *Pulp and Paper Magazine of Canada*, **66**: T407–T414 (1965).
33. Merchant, M.V., "A study of water-swollen cellulose fibers which have been liquid exchanged and dried from hydrocarbons", *Tappi J*., **40**: 771–781 (1957).
34. Duchesne, D., Daniel, G., "Changes in surface ultrastructure of Norway Spruce fibres during kraft pulping – visualization by field emission-SEM, *Nord. Pulp Pap. Res. J*., **15**: 54–61 (2000).

35. Hanley, S.J., Gray, D.G., "AFM image in air and water of kraft pulp fibers", *J. Pulp Pap. Sci*., **25**: 196–200 (1999).
36. Donaldson, L.A., Singh, A.P., "Bridge-like structures between cellulose microfibrils in Radiata Pine (*Pinus radiata D. Don*) kraft pulp and holocellulose", *Holzforschung*, **52**: 449–454 (1998).
37. Weatherwax, R.C., Caulfield, D.F., "Cellulose aerogels: and improved method for preparing a highly expanded form of dry cellulose", *Tappi J*., **54**: 138–139 (1971).
38. Plouchly, J., Biros, J., Benes, S.: Makromol. Chem., **180**: 745–760 (1979).
39. Berlin, E., Kliman, P.G., Pallansch, M.J., "Changes in the state of water in proteinaceous systems", *J. Colloid Interface Sci.,* **34**: 488–494 (1970).
40. Li, T., "Interactions Between Water and Cellulose Fibers, Application of NMR Techniques", Doctoral Thesis, Royal Institute of Technology, Stockholm (1991).
41. Page, D.H., "The beating of chemical pulps – the action and the effects", Fundamentals of Papermaking, Transactions of the Ninth Fundamental Research Symposium Held at Cambridge, 1–38 (1989).
42. Scallan, A.M., "The accommodation of water within pulp fibers", Fiber-Water Interactions in Paper-Making, Transactions of the Symposium, Oxford, 9–27 (1978).
43. Mason, G., "Porous materials and percolation theory: Characterization of Porous Solids", Bad Soden, Germany, 323–332 (1988).
44. Eyraud, C., Quinson, J.F., Brun, M., "The role of thermoporosimetry in the study of porous solids: Characterization of Porous Solids", Bad Soden, Germany, 295–305 (1988).
45. Quinson, J.F., Brun, M., "Progress in thermoporosimetry: Characterization of Porous Solids, Bad Soden, Germany, 307–315 (1988).
46. Nenow, D., Trayanov, D., "Surface melting of small crystals", *J. Crystal Growth*, **99**: 102–105 (1990).

Transcription of Discussion

THERMOPOROSIMETRY OF PULP FIBERS

Thad C. Maloney[1] *and Hannu Paulapuro*[2]

[1]JM Huber Finland Oy
[2]HelsinkiUniversity of Technology

John Roberts Department of Paper Science, UMIST

A significant part of the cell wall is made of highly hydrated non-cellulosic polysaccharides xylans, xyloglucans, arabinoxylans etc., I wonder how the technique that you use deals with the water of hydration of these polymers. When you exchange to cyclohexane these would not be solvated in any way, so does this account for some of the differences that you have observed between the cyclohexane and the water results?

Thad Maloney

This is a really important question but unfortunately I really don't have a good answer for it. I know that the hydration of the polymer is not desirable for my measurement, because it influences on the measured pore size distribution. The essential assumption in my technique is that the pore structure of the cylcohexane saturated fibres is largely preserved and reflects the pore structure of water swollen fibres.

Lars Wågberg Mid-Sweden University

You describe a difference between the fibre saturation point and the thermoporosimetry. My explanation to this difference is that you have not tested polymers as large as 700 nanometers. If you could find a polymer of 700 nanometers you might find pores in that size range as well. If you look at dextrans or the other polymers you were using they are far from 700 nanometers. Have you tried to find those kinds of polymers. Maybe you would find the pore volume in this size range if you tried them?

Thad Maloney

No I haven't tried them, but it is a very good idea.

Warwick Raverty CSIRO Australia

To what extent is the damage that you observe in the micropore structure in water caused by the fact that water expands when it freezes?

Thad Maloney

Well I think that pore damage arises basically through two mechanisms, one is de-hydration. Crystals form on the outside of the fibre wall and simply de-hydrate the fibre. This is indicated by the loss in fibre saturation point. I think the experiments that I have done in which the water on the outside of the pulp fibres was kept frozen and repeatedly melted and frozen the water inside the cell wall indicate that there is also internal damage. In other words, crystals inside the cell wall grow and expand and destroy the cell wall. I would like to refer to a paper by Paul Kibblewhite who has studied the effect of freezing on pulp fibres. You can see in his microscopic analysis that freezing causes major damage to pulp fibres.

John Parker Consultant

Can you deduce anything from the fact in Figure 12 you get straight lines when you plot pore volume against the logarithm of pore diameter. Does this convey anything to you about the structure?

Thad Maloney

No I really don't know what the significance is of that.

Ian Parker APPI/Monash University

If you think about the size of the fibre wall and how much swelling takes place in water, there doesn't seem to be enough space for 700 nanometers. Is it possible that you are actually looking at the lumen?

Thad Maloney

No I am not looking at the lumen because I have made measurements on

dried pulp, so I can see the effect of the lumen in those. The lumen is a very big pore, it is far outside the measurement range.

Ian Parker

700 Nanometers is huge, it is the thickness of the fibre wall.

Thad Maloney

Yes I agree, it is a big pore, but look at the experiment, look at the very good agreement with mercury porisimetry. It is an accurate technique and it is showing 700 nanometer pores, that is the mystery. Really we are going to have to solve that. I understand your concerns completely, but this is what the data shows.

Derek Page Institute of Paper Science & Technology

You say in your text it has sometimes been postulated that there is a class of pore above one micron in diameter which is formed in the cell wall of chemical pulp during refining. It is more than a postulate. You can take a fibre that has been beaten, put it under a microscope slide, still in water, and you can see using light microscopy that there are very large holes in the cell wall. They are often as large as a micron or two microns in diameter. Sometimes in fact they are as large as the lumen. What you can't do very easily by microscopy is to quantify them of course. You haven't been able to quantify them either. However they have been shown to be present by a number of techniques and by a number of different authors.

Thad Maloney

Excuse my rather weak language I agree completely that they are there and my original motivation in developing the cyclohexane technique was to measure these. That was what I was really trying to do when I started out. I couldn't push the range of my measurement up high enough, when I tried to push the range of the measurement even higher I had some indication that they were there, but I didn't feel comfortable enough with the data to come here and present it. But I agree that they are there, and I want to measure them.

Peter Herdman Arjo Wiggins

Yes I agree entirely with Derek Page, if you look at the very first proceedings you will even see fibre ballooning pictures with enormous pores. The other thing that I might point out is that these pores aren't spherical or anything like spherical. Perhaps the 700 nanometer dimension that we are measuring is actually running along the length of the fibre and the morphology of these pores could be extremely complex, so when you are saying that you are measuring a range of micropores maybe you are making a lot of dimensional measurements on one large topographically peculiar micropore. Furthermore because the separation of the two surfaces of the micropore are not uniform you would not expect to see a uniform diffraction pattern with a probe like slow neutron scattering one. Perhaps this is why we don't observe these large pores with some of the work that Ian Parker was reporting earlier, and yet you can see it when you are looking at a volumetric fractional measurement. Do you think that your volumetric fractional measurement compared to a number count of distances between lamellae account for some of the observations that we have seen?

Thad Maloney

I agree completely that it is a very complex issue to try to relate the Gibbs-Thompson radius of curvature to the actual separation of microfibrils. Remember that the basis of my data is the measurement on porous glasses, and then I make a very simple assumption about the pore geometry, and then measure pulp fibres. In reality the pore structure of the cell wall has a different geometry than porous glass. For example the pores are spaces between microfibrils so they are convex rather than concave. This influences the melting temperature depression. Certainly this simple model of cylindrical pores isn't so good and I think that this why I measure 700 nanometer pores. The next step we will have to take is to study porous substances with differing geometries, and to try to work out a more complex model that more closely resembles the cell wall.

Ian Parker

With small angle neutron scattering the analysis at small g (small scattering angles), the region of scattering of large pores, only gives a mean size, not a distribution. It was also carried out on fibres at equilibrium with various RH atmospheres, unlike Thad Maloney's fibres which were saturated in water. The neutron beam was also normal to the fibres so would not see any longitudinal pores.

Gary Baum Institute of Paper Science & Technology

All this work was on undried fibres, do you plan to look at once dried fibres?

Thad Maloney

There are a few results on once dried fibres in the paper. We are using this method today to look at hornification and also to look at beating of once dried pulps. The results from this work are very encouraging.